

Electron spin relaxation in bulk GaAs for doping densities close to the metal-to-insulator transition

M. Römer,^{1,*} H. Bernien,¹ G. Müller,¹ D. Schuh,² J. Hübner,¹ and M. Oestreich^{1,3}

¹*Institute for Solid State Physics, Gottfried Wilhelm Leibniz University of Hannover, Appelstr. 2, 30167 Hannover, Germany*

²*Institute for Experimental and Applied Physics,
Regensburg University, D-93040 Regensburg, Germany*

³*Centre for Quantum Engineering and Space-Time Research (QUEST), Hannover, Germany*

(Dated: June 15, 2018)

We have measured the electron spin relaxation rate and the integrated spin noise power in n-doped GaAs for temperatures between 4 K and 80 K and for doping concentrations ranging from $2.7 \times 10^{-15} \text{ cm}^{-3}$ to $8.8 \times 10^{-16} \text{ cm}^{-3}$ using spin noise spectroscopy. The temperature dependent measurements show a clear transition from localized to free electrons for the lower doped samples and confirm mainly free electrons at all temperatures for the highest doped sample. While the sample at the metal-insulator-transition shows the longest spin relaxation time at low temperatures, a clear crossing of the spin relaxation rates is observed at 70 K and the highest doped sample reveals the longest spin relaxation time above 70 K.

PACS numbers: 61.72.sd, 72.25.Rb

I. INTRODUCTION

Non-equilibrium electron spin relaxation in semiconductors has been studied for nearly forty years and is today in the focus of intense research due to the vision of semiconductor spintronic devices. The most prominent model system in this field is n-doped bulk GaAs since high quality GaAs is easily available and spin polarized electrons can be efficiently excited and detected by circularly polarized light excitation and photoluminescence detection. An excellent overview about the most relevant spin relaxation mechanisms and experimental results in this material system is given in Refs. 1,2,3. Presently the non-equilibrium electron spin relaxation in n-doped GaAs is perfectly understood for low temperatures and doping concentrations well above the metal-to-insulator transition (MIT) where the Dyakonov-Perel (DP) spin relaxation dominates. The same is true for all doping concentrations at high temperatures⁴ where all electrons are delocalized and the spin dynamics can be well described by semiconductor spin Bloch equations⁵. The situation becomes much more complex for the doping regime at the metal-to-insulator transition at low temperatures where the spin relaxation times turn out to be very long. In this regime, the theoretical description becomes more complicated due to the intricate interplay of localized and free electrons. At the same time, the experiments become more difficult since optical excitation changes momentum scattering times and the ratio of free and localized electrons.

The most detailed work on the non-equilibrium, low temperature electron spin relaxation time in dependence on doping density has been performed by Dzhioev et al.². They identified hyperfine interaction, anisotropic exchange interaction, and the DP mechanism as the dominant spin relaxation mechanisms for doping densities below $2 \times 10^{15} \text{ cm}^{-3}$, between $2 \times 10^{15} \text{ cm}^{-3}$ and the MIT,

and above the MIT, respectively. Dzhioev et al. have measured the non-equilibrium spin relaxation by optical Hanle depolarization experiments and consequently observed a strong dependence of the spin relaxation time on excitation power. In this publication, we complement their experiments and measure the *equilibrium* spin relaxation time by nearly perturbation free spin noise spectroscopy for different doping concentrations over a wide temperature range.

II. SAMPLES AND EXPERIMENTAL SETUP

The samples are one 2 μm thick, silicon-doped, molecular-beam epitaxy (MBE) grown GaAs sample with AlGaAs barriers with a doping concentration of $n_D = 1 \times 10^{14} \text{ cm}^{-3}$ (sample A^{v1}; very low doped) and three silicon-doped, Chocharalskii-grown, GaAs wafers with doping concentrations of $n_D = 2.7 \times 10^{15} \text{ cm}^{-3}$ (sample B^{low}; low doped), $n_D = 1.8 \times 10^{16} \text{ cm}^{-3}$ (sample C^{MIT}; doping close to the MIT), and $n_D = 8.8 \times 10^{16} \text{ cm}^{-3}$ (sample D^{high}; high doping concentration). All samples are equipped with a high quality, $\lambda/4$ silicon nitride antireflection coating. For transmission experiments, the MBE grown GaAs/AlGaAs layer has been lift-off from the GaAs substrate and Van-der-Waals bonded to a sapphire substrate.

Figure 1(a) depicts the experimental spin noise spectroscopy setup.⁶ The light source is a low noise, tunable diode laser in Littmann configuration. A Faraday isolator avoids feedback into the laser and a single mode fibre is used as spatial filter to ensure a Gaussian spatial laser profile. The laser light is focused to a beam waist of $w_0 = 80 \mu\text{m}$ in the sample which is mounted in a He cold finger cryostat. The wavelength of the linearly polarized laser light is tuned below the GaAs band gap to avoid laser light absorption. The GaAs donor electrons are in thermal equilibrium with zero mean spin polariza-

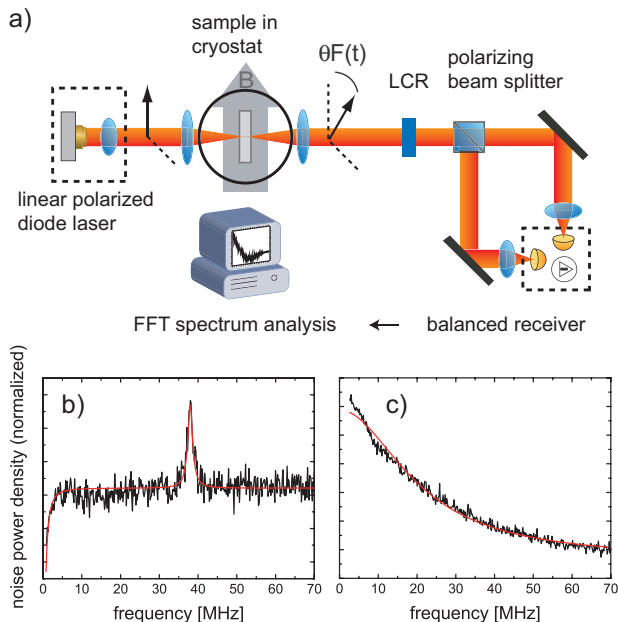


FIG. 1: (a) Spin noise spectroscopy setup. The external magnetic field shifts the center frequency of the spin noise signal by the electron Larmor frequency. (b) Typical spin noise spectrum acquired by subtracting spin noise spectra measured at $B=6$ and 0 mT for sample C^{MIT} at 4 K. (c) Typical spin noise difference spectrum acquired by selective suppression of spin noise with a liquid crystal retarder for sample B^{low} at 10 K.

tion but the temporal statistical fluctuations of the spin polarization are unequal to zero and yield a fluctuating Faraday rotation of the linear laser light polarization. This Faraday rotation is measured by a combination of a polarizing beam splitter and an 80 MHz balanced photoreceiver. The electrical signal is amplified by a low noise amplifier and passed through a 67 MHz low pass filter. The fluctuation signal is digitized with 180 MS/s and 16 bit in the time domain and Fourier transformed in real time. To eliminate the white photon shot noise in the measured spectra, a second spin noise spectrum with the spin noise either shifted in frequency or totally suppressed is acquired and subtracted. Figure 1(b) shows a typical difference spectrum obtained by subtracting two spectra acquired at $B = 6$ and 0 mT, respectively, i.e., the second of the two spin noise spectra has been shifted by the electron Larmor frequency. Figure 1(c) shows a typical difference spectrum acquired by selective spin noise suppression. The selective suppression of the noise signal is performed by a liquid crystal retarder (LCR) after the cryostat with the fast axis aligned parallel to the polarization plane of the laser. The LCR can be set to retardance of $\lambda/4$ (spin noise suppressed) or $\lambda/2$ (no change). When possible both methods are combined in a double difference technique to eliminate remaining offsets, e.g., due to a slightly different transmission of the LCR for $\lambda/2$ and $\lambda/4$ retardation.

To assess the influence of unwanted residual optical excitation or time-of-flight broadening on the measured

spin relaxation time, the laser spot diameter has been varied from $30 \mu\text{m}$ to $120 \mu\text{m}$ while keeping the total laser power constant. Enlarging the focus spot reduces the power density in the sample and time-of-flight broadening, i.e., minimizes spurious effects due to the measurement technique⁷. The interrelation of the energy position of the probe light relative to the electronic resonance has been studied previously⁶. The optimum results have been obtained for a probe laser wavelength of 840 nm, 4 mW power, and $80 \mu\text{m}$ spot size. Longer wavelengths, lower laser power, or larger spot diameters did not change the measured spin relaxation times but reduced the signal to noise ratio significantly thus increasing the required averaging time. Different measurement conditions have been used for sample A^{vl} as the short spin lifetime and the low donor concentration lead to a small noise signal at large laser detuning. The sharp excitonic lines at low temperatures and low dopand concentration allow the use of a laser wavelength of 820.7 nm with only negligible absorption.

III. EXPERIMENTAL RESULTS

In the following we present the temperature dependence of the spin relaxation rate Γ_s and of the spin noise power P_s and discuss the influence of free and localized electrons on the spin relaxation. The samples can be classified into three categories by their doping concentration namely the completely localized phase (sample A^{vl}), the metallic phase (sample D^{high}), and the mixed phase around the MIT (samples B^{low} and C^{MIT}). Figure 2(a) shows the temperature dependence of the spin relaxation rate Γ_s for sample B^{low} , C^{MIT} , and D^{high} in the temperature range from 4 K to 80 K and for sample A^{vl} at 8 K.

A. Metallic phase

The doping of the highest doped sample D^{high} is well above the MIT and the conduction band is populated even at very low temperatures due to the hybridization of impurity and conduction band, i.e., all electrons are delocalized, the Fermi level is at low temperatures well in the conduction band, the dominant spin relaxation mechanism is the DP mechanism, and ionized impurity scattering is the main electron scattering mechanism. The delocalization is substantiated by the temperature dependence of the integrated spin noise power (see Fig. 2(b)) which extrapolates to zero noise power at zero temperature due to spin Pauli blockade. In the range from 30 K to 80 K the temperature dependence is proportional to $T^{1.48 \pm 0.06}$ which is in very good agreement with the expected $T^{3/2}$ dependence in the case of charged impurity scattering⁸. Also the low temperature value of Γ_s measured by SNS is in rather good agreement²⁴ with the Hanle measurement by Dzhiyev et al.². Such an agreement is expected since the influence of the weak optical

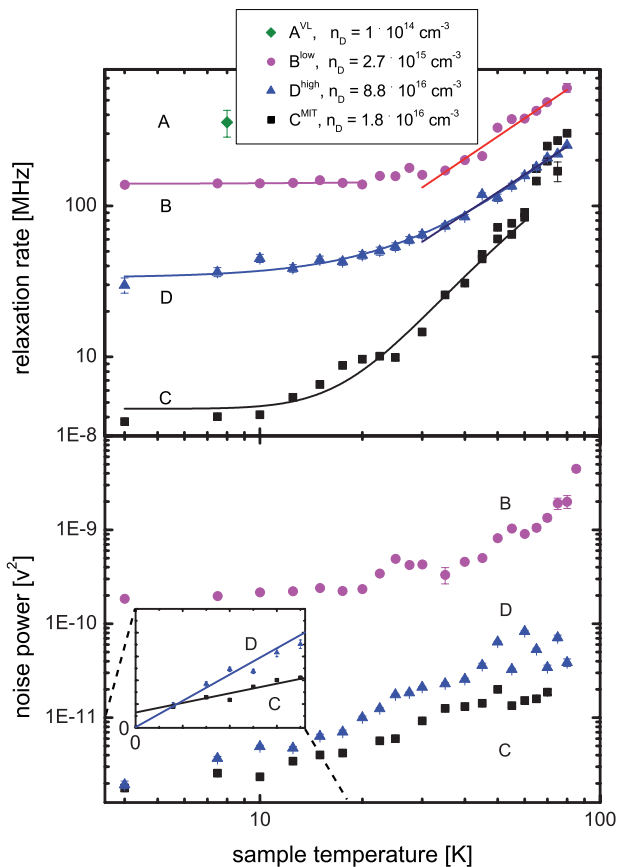


FIG. 2: (a) Temperature depended measurement of the spin relaxation rate for the samples B-D using a large focus and a large detuning of the laser wavelength from the optical transitions (probe laser wavelength $\lambda = 840$ nm) and the spin relaxation rate for sample A at 8 K. The solid lines are fits to the data. The fit parameters are listed in table I. (b) Temperature dependence of the integrated spin noise power for samples B-D. The noise powers have been scaled to account for the different thicknesses of the samples. The inset shows the low temperature noise power for samples C and D on a linear scale.

excitation in the Hanle experiment is small for this doping concentration.

B. Non-interacting donors

The other extreme concerning doping is sample A^{vl} where the average distance between two donors is more than 200 nm. The electrons are at low temperatures completely localized at the donor atoms and electron-electron interaction can be neglected in good approximation. The dominant spin relaxation is in this case hyperfine interaction with nuclear spins which can be expressed by an effective nuclear magnetic field B_N . The strength and direction of B_N varies at thermodynamic equilibrium stochastically from donor to donor resulting in a dephasing of the ensemble electron spin polarization

due to an inhomogeneous Larmor precession. The measured spin relaxation time in sample A^{vl} is $2.8(\pm 0.7)$ ns (8 K²⁵) which is in fair agreement with the calculated value of 3.6 ns by Merkulov et al.⁹. Following the calculations of Merkulov et al. one third of the electrons, i.e., electrons with spins aligned along B_N , show orders of magnitudes longer spin relaxation times when no external magnetic field is applied. In the thin sample A^{vl} we do not observe such long τ_s since the free exciton line is broadened due to strain and the resulting residual absorption prevents the detection of such very long spin dephasing times. The free (bound exciton) resonance is inhomogeneously broadened by 0.9 meV (3 meV) due to inhomogeneous strain in the lift-off sample which results in residual light absorption. The residual light absorption can not be avoided in this sample by longer laser wavelengths due to a scarce signal-to-noise ratio. The light absorption leads to the creation of trions which suppress spin noise by Pauli blockade, i.e., the by SNS measured τ_s is a lower bound. In contrast, the optical non-resonant excitation in Hanle experiments yields free carriers which lead to an increased averaging of the the hyperfine interaction and hence a decrease of the spin relaxation rate¹⁰, i.e., Hanle experiments give in first approximation an upper bound for τ_s . However, the intricate density dependence at very low densities complicates the interpretation of Hanle experiments and a linear extrapolation of τ_s to zero excitation is ambiguous. The spin relaxation time τ_s measured by SNS is by a factor of two smaller than the value measured by Dzhioev et al. by the Hanle effect², which we attribute to the reasoning pointed out above. The large relative error bar of τ_s for sample A^{vl} compared to the other samples is due to the fact that the spin noise spectrum is broader than the detection bandwidth of the setup which complicates the data analysis. We have not measured the temperature dependence of τ_s for this sample since ionization of the donor bound electrons increases significantly above 10 K (see Fig. 3).

C. Mixed phase

The height of the localization potential and degree of localization for samples close to the metal insulator transition delicately depend on the donor concentration and temperature. For lower doping concentrations the localization potential is higher, electron-electron interaction is weaker, and delocalization occurs besides the higher localization potential at lower temperatures.

Figure 2 shows inter alia the temperature dependence of Γ_s and P_s for the second lowest doped sample B^{low} . Both are approximately constant for temperatures up to 20 K which is consistent with localized electrons. At low temperature τ_s is longer than in sample A^{vl} which results from the exchange interaction between the donor electrons,¹² i.e., the spin interaction causes an effective averaging over the locally different nuclear fields which increases τ_s . Interestingly, $\tau_s = 7$ ns measured by SNS is

sample	spin relaxation rate	temperature regime
A ^{vl}	$\Gamma_s = 357 \pm 72$ MHz	T = 8 K
B ^{low}	$\Gamma_s = 140 \pm 2$ MHz	T = 4..20 K
B ^{low}	$\Gamma_s \propto T^{1.48 \pm 0.09}$	T = 30..80 K
C ^{MIT}	$\Gamma_s = 3065$ MHz $\times \exp(-(1028 \text{ K}/T)^{1/2}) + 4.5$ MHz	T = 4..60 K
D ^{high}	$\Gamma_s \propto T^{1.48 \pm 0.06}$	T = 30..80 K
D ^{high}	$\Gamma_s = 0.04$ MHz $\times (T/\text{K})^{1.96 \pm 0.08} + 33.5$ MHz	T = 2..80 K

TABLE I: Temperature dependence of the spin relaxation rates from fits to Γ_s from Fig. 2(a).

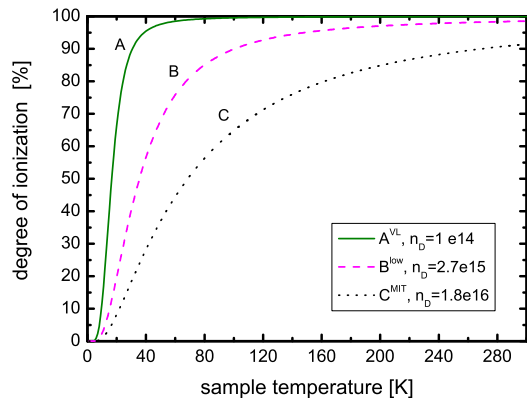


FIG. 3: Temperature dependence of the degree of electron ionization for the three lowest doped samples calculated by Blakemore’s equation¹¹. The validity of Blakemore’s equation decreases with increasing doping concentration due to the formation of impurity bands, i.e., the calculation for sample C is only of limited significance.

significantly shorter than τ_s measured by Hanle experiments where τ_s varies for comparable doping concentrations between ~ 26 ns (Colton et. al.¹³) and ~ 180 ns (Dzhioev et al.²). This large spread of the values of τ_s can only partially be explained by the strong dependence of τ_s on the exact doping concentration, the ratio of compensation, and the purity of the individual sample. Most probably, the longer spin relaxation times observed via the Hanle effect are again at least to some extent – as for doping concentrations of 10^{14} cm^{-3} – due to optical excitation¹⁴.

At this point, we want to overcome a recent misleading statement against SNS which results from a very commendable and detailed comparison of Hanle and SNS by Crooker et al.¹⁵. The authors state that SNS is by no means a panacea and that accurate measurements of τ_s are more readily and quickly obtained using conventional techniques based on the Hanle effect, which is particularly correct for higher doping concentrations and elevated temperatures. However, Figure 5 of Ref. 15 implies to non-experts that the Hanle technique is superior to SNS and less perturbative, which does not hold in general. As

stated in Ref. 15, SNS is nonperturbative for long wavelengths, however the shorter spin relaxation time results from time-of-flight broadening which is known from experiments on atomic gases¹⁶ and has recently been verified for the first time in semiconductor quantum wells⁷. This effect is absent for localized carriers and can be overcome by a sufficiently large laser spot for free carriers.

Figure 2 also shows for sample B^{low} an increase of Γ_s for temperatures above 30 K which is proportional to $T^{1.48 \pm 0.09}$. This increase of Γ_s results from ionization of the electrons and efficient spin relaxation of the ionized electron spins due to the DP spin relaxation mechanism. According to Blakemore’s formula, the degree of ionized electrons at 30 K is about 50 % and the percentage rises by 1.5 % per Kelvin at this doping concentration, i.e., spin relaxation by nuclear hyperfine interaction can be neglected above 30 K since the efficiency of DP increases with temperature and the efficiency of spin relaxation by hyperfine interaction decreases due to the interaction of localized and free electrons and the resulting efficient averaging over the nuclear fields.

D. Close to the metal-to-insulator transition

Sample C^{MIT} has a donor concentration right at the MIT which occurs for GaAs at a concentration of $n_D \approx 2 \times 10^{16} \text{ cm}^{-3}$. The MIT is characterized by overlapping donor atoms which start to form an impurity band below the conduction band¹⁷ and allows electrical conductivity over macroscopic distances by percolation paths, i.e., the low temperature Fermi level is located inside the impurity band¹⁸, such that some electrons are completely delocalized but most electrons are confined on a macroscopic scale but therein delocalized. Figure 2(b) shows that P_s decreases for decreasing temperature but does not completely vanish for extrapolation to zero temperature which substantiates partial Pauli spin blockade. The overall spin noise power is smaller for sample C^{MIT} compared to sample D^{high} due to the lower electron density in sample C^{MIT} and is also smaller compared to the lower doped sample B^{low} due to strong excitonic enhancement of the spin noise signal in sample B^{low} even at moderate temperatures.

The squares in Fig. 2(a) depict the temperature de-

pendence of Γ_s for sample C^{MIT}. We observe a long spin relaxation time of 267 ns at 4 K which is about 200 ns longer than the value reported in Ref. 2 for a similar sample. The sample has the longest τ_s at low temperatures but Γ_s increases strongly for temperatures above 10 K. Above 70 K, Γ_s of sample C^{MIT} becomes larger than Γ_s of the highly doped sample D^{high}, i.e., samples at the metal-to-insulator transition have only the longest spin relaxation times at low temperatures but not at high temperatures. This crossing of Γ_s at finite temperatures is not surprising since the Fermi distribution becomes a Maxwell-Boltzmann distribution and hence the average electron energy becomes independent of doping concentration. At the same time, electron-electron and electron-impurity scattering are faster for higher doping concentrations which leads to a more efficient motional narrowing and less efficient spin relaxation by the DP mechanism. Simple estimations of Γ_s by the DP mechanism using the Brooks-Herring approach for charged impurity scattering confirm theoretically the crossover of Γ_s at $T \approx 70$ K for sample C^{MIT} and D^{high}. We estimate that for free electrons and carrier temperatures above the Fermi temperature (E_F/k_B) the sample with the highest doping concentration shows the longest spin dephasing time.

Up to temperatures of 60 K, Γ_s of sample C^{MIT} does not follow the usual temperature dependence of the DP spin relaxation mechanism calculated by scattering of free electrons at charged impurities. In fact, we have measured the conductivity σ versus temperature which is up to a temperature of 60 K well described by hopping transport with $\sigma = \sigma_0 \exp(-(T_0/T)^{1/2}) + \sigma_m$ as shown in Fig. 4(a). The exponential term describes the hopping transport and σ_m is a metal-like contribution to the conductivity¹⁹. For temperatures higher than 60 K, most electrons are delocalized and the sample shows normal metallic conductivity. In Fig. 4(b)) a fit with the same temperature dependence ($\Gamma_s = \Gamma_0 \exp(-(T_0/T)^{1/2}) + \Gamma_m$) and the same value for T_0 has been applied to the spin relaxation rate showing that Γ_s is proportional to the conductivity.

Spin relaxation in the hopping regime can occur via a DP like spin relaxation mechanism as described by Shklovskii^{12,20} or via anisotropic spin exchange (Dzyaloshinskii-Moriya^{21,22} interaction (DM)) as described by Kavokin²³. Putikka et al.¹⁴ estimate the spin relaxation rate due to the DM mechanism by

$$\Gamma_{DM} = 1/\tau_{DM} = \alpha_{DM} N_D a_B^3 f_{DM}(T), \quad (1)$$

where $a_B = 10.6$ nm is the Bohr radius of the bound electron, $\alpha_{DM}(\text{th}) = 0.01 \text{ ns}^{-1}$ (theoretical value) or $\alpha_{DM}(\text{exp}) = 0.03 \text{ ns}^{-1}$ (experimental value) is a constant relaxation rate, and $f_{DM}(T) \approx 32$ at $T = 5$ K is a weakly temperature-dependent function. Accordingly, we calculate for sample C^{MIT} at 5 K a spin relaxation time in the range of $\tau_{DM}(\text{th}) \approx 150$ ns and $\tau_{DM}(\text{exp}) \approx 485$ ns, which is consistent with the measured value of 267 ns.

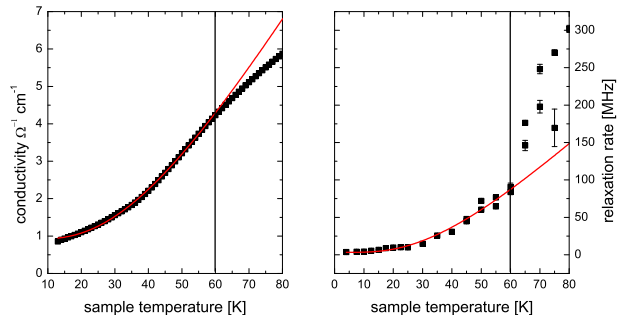


FIG. 4: Temperature dependence of the spin relaxation in the hopping regime depends on the conductivity. Hopping transport describes the temperature dependence well for temperatures below 60 K.

IV. SUMMARY

The temperature dependence of the electron spin relaxation time τ_s in bulk n-GaAs has been studied using spin noise spectroscopy. The results are summarized in Table I. The different samples with doping concentrations in the vicinity of the metal-to-insulator transition cover the range from fully localized to entirely free electrons which is confirmed by temperature dependent measurements of the spin noise power. At high temperatures, all measurements are consistent with DP spin relaxation of free electrons. At low temperatures and low doping concentrations, τ_s is in good approximation independent of temperature since the electrons are localized. At the same time, τ_s measured by spin noise spectroscopy is shorter than in comparable measurements by the Hanle technique which can be attributed to weaker perturbation in the case of SNS. For doping densities at the metal-to-insulator transition and temperatures up to 60 K, both conductivity and τ_s are well described by hopping transport. Interestingly, the low temperature spin relaxation time is longest for doping densities at the metal-to-insulator transition but Γ_s increases with temperature less rapidly for higher doped samples. At 70 K, a crossing of Γ_s appears for the two doping concentrations $n_D = 1.8 \times 10^{16} \text{ cm}^{-3}$ and $n_D = 8.8 \times 10^{16} \text{ cm}^{-3}$ and τ_s of the higher doped sample becomes longer than τ_s for the lower doped sample. This crossing results mainly from the transition from Fermi-Dirac to Maxwell-Boltzmann electron distribution and the faster electron momentum scattering by charged impurities in the higher doped sample.

V. ACKNOWLEDGEMENT

This work was supported by the German Science Foundation (DFG priority program 1285 ‘Semiconductor Spintronics’), the Federal Ministry for Education and

Research (BMBF NanoQuit), and the Centre for Quantum Engineering and Space-Time Research in Hannover

(QUEST). G.M.M. acknowledges support from the Evangelisches Studienwerk.

-
- * Electronic address: roemer@nano.uni-hannover.de;
URL: <http://www.nano.uni-hannover.de/>
- ¹ F. Meier and B. P. Zakharchenya (eds.), *Optical Orientation* (Elsevier, Amsterdam, 1984).
 - ² R. I. Dzhioev, K. V. Kavokin, V. L. Korenev, M. V. Lazarev, B. Y. Meltser, M. N. Stepanova, B. P. Zakharchenya, D. Gammon, and D. S. Katzer, Phys. Rev. B **66**, 245204 (2002).
 - ³ M. I. Dyakonov (ed.), *Spin Physics in Semiconductors*, volume 157 of *Solid-State Sciences* (Springer-Verlag, 2008).
 - ⁴ S. Oertel, J. Hübner, and M. Oestreich, Appl. Phys. Lett. **93**, 132112 (2008).
 - ⁵ J. H. Jiang and M. W. Wu, Phys. Rev. B **79**, 125206 (2009).
 - ⁶ M. Römer, J. Hübner, and M. Oestreich, Rev. Sci. Instrum. **78**, 103903 (2007).
 - ⁷ G. M. Müller, M. Römer, D. Schuh, W. Wegscheider, J. Hübner, and M. Oestreich, Phys. Rev. Lett. **101**, 206601 (2008).
 - ⁸ I. Žutić, J. Fabian, and S. D. Sarma, Rev. Mod. Phys. **76**, 323 (2004).
 - ⁹ I. A. Merkulov, A. L. Efros, and M. Rosen, Phys. Rev. B **65**, 205309 (2002).
 - ¹⁰ M. Furis, D. L. Smith, S. A. Crooker, and J. L. Reno, Appl. Phys. Lett. **89**, 102102 (2006).
 - ¹¹ J. S. Blakemore, *Semiconductor Statistics* (Dover Publications, 2002).
 - ¹² K. V. Kavokin, Semicond. Sci. Technol. **23**, 114009 (2008).
 - ¹³ J. S. Colton, T. A. Kennedy, A. S. Bracker, and D. Gammon, phys. stat. sol. (b) **233**, 445 (2002).
 - ¹⁴ W. O. Putikka and R. Joynt, Phys. Rev. B **70**, 113201 (2004).
 - ¹⁵ S. A. Crooker, L. Cheng, and D. L. Smith, Phys. Rev. B **79**, 035208 (2009).
 - ¹⁶ S. A. Crooker, D. G. Rickel, A. V. Balatsky, and D. L. Smith, Nature **431**, 49 (2004).
 - ¹⁷ R. A. Abram, G. J. Rees, and B. L. H. Wilson, Adv. Phys. **27**, 799 (1978).
 - ¹⁸ B. I. Shklovskii and A. L. Efros, *Electronic Properties of Doped Semiconductors*, volume 45 of *Solid-State Sciences* (Springer-Verlag, 1984).
 - ¹⁹ M. Benzaquen, D. Walsh, and K. Mazuruk, Phys. Rev. B **36**, 4748 (1987).
 - ²⁰ B. I. Shklovskii, Phys. Rev. B **73**, 193201 (2006).
 - ²¹ T. Moriya, Phys. Rev. **120**, 91 (1960).
 - ²² I. Dzyaloshinsky, J. Phys. Chem. Solids **4**, 241 (1958).
 - ²³ K. V. Kavokin, Phys. Rev. B **64**, 075305 (2001).
 - ²⁴ The discrepancy might result from the higher impurity concentration and a resulting faster momentum scattering time in our Chochralskii-grown GaAs.
 - ²⁵ Sample A^{VI} has been measured in a helium free cryostat, where 8 K was the minimum temperature.